Cyclen-based bismacrocycles for biological anion recognition. A potentiometric and NMR study of AMP, ADP and ATP nucleotide complexation†

Anne-Sophie Delépine, Raphaël Tripier and Henri Handel*

Received 18th December 2007, Accepted 7th March 2008
First published as an Advance Article on the web 26th March 2008
DOI: 10.1039/b719514a

The behaviour of two cyclen-based bismacrocycles linked by aromatic spacers as receptors of adenosine monophosphate (***AMP***), adenosine diphosphate (***ADP***) and adenosine triphosphate (***ATP***) anions is explored. The two bismacrocycles differ from one another by the nature of their spacers, which are respectively 1,3-dimethylbenzene (***BMC***), or 2,6-dimethylpyridine (***BPyC***). Potentiometric investigations supported by ^{1}H and ^{31}P NMR measurements were performed over a wide pH range to characterize and understand the driving forces implicated in the supramolecular assemblies. A comparison is also carried out with the results presented in this work and those obtained previously with these two ligands and inorganic phosphates. The comparison exhibits the importance of π-stacking capability of the organic anions in the binding and hydrogen-bonding network. For ***BPyC***, NMR studies highlight two coordination schemes depending on the protonation of the nitrogen atom of the pyridinyl spacer, which acts in acidic media as a supplementary anchoring point.

Introduction

The chemistry of anion recognition has rapidly grown in recent decades to become an important area of supramolecular chemistry owing to the presence of multiple and various anionic species in both inorganic applications and biological systems.[1–10] For instance, a large variety of substrates and cofactors engaged in biological processes such as nucleotides are negatively charged and present specific properties that have to be taken into account in order to propose adequate receptors. The strategies developed to obtain efficient "host–guest" interactions with anions mainly consists in the use of coordinative interactions with metal ions included in the ligand or, alternatively, *via* non-covalent interactions with binding sites of the receptor, namely coulombic forces, hydrogen bonding and π-stacking interactions. In this last case, polyammonium groups have proved to be very efficient, and among them, polyprotonated macrocycles behave as effective receptors for polycharged phosphate anions in aqueous solutions: they strongly associate to nucleotides *via* multiple interactions with the negatively charged polyphosphate chain.[8,9] Another important requirement consists in the correspondence between the binding sites of the receptor and those of the substrate. Consequently, the favourable arrangement of the different components involved in the recognition process constitutes a fundamental condition for high binding constants.

In previous papers, we demonstrated that protonated cyclen-based bismacrocycles as ***BMC*** and ***BPyC*** (Fig. 1) are able to form very stable ternary species with inorganic polyphosphate anions, particularly the triphosphate, due to the localization of the nitrogen atoms concerned with the ternary species formation and, among others, the participation of the pyridinyl linker.[11]

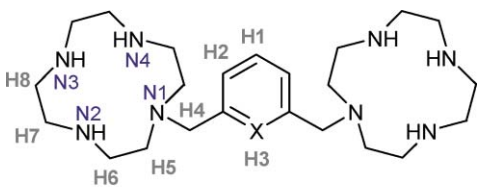

BMC (X = CH) and ***BPyC*** (X = N)

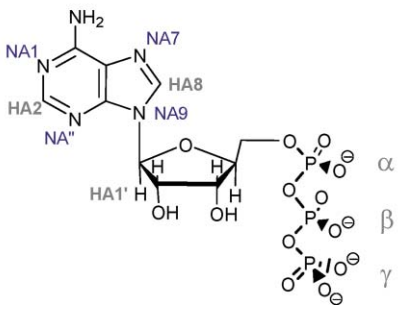

Fig. 1 The two studied host ligands (top) and ***ATP*** (bottom).

We present here a study of the recognition phenomena that take place between the ***BMC*** and ***BPyC*** bismacrocycles and adenosine monophosphate (***AMP***), adenosine diphosphate (***ADP***) and adenosine triphosphate (***ATP***) anions, based on potentiometric equilibrium methods. In order to obtain supplementary

UMR CNRS 6521, "Chimie, Electrochimie Moléculaire et Analytique", Université de Bretagne Occidentale, C. S. 93837, 6 avenue Victor Le Gorgeu, 29238, Brest, Cedex 3, France. E-mail: Henri.Handel@univ-brest.fr; Fax: +33 2 98016138; Tel: +33 2 98017001

† Electronic supplementary information (ESI) available: Distribution diagrams for ternary systems with AMP and ADP; logarithm recognition constants and experimental ^{1}H chemical shifts with the corresponding inorganic phosphates; crystal structure data for $BPyCH_7^{7+}$ (CCDC reference number 671278). See DOI: 10.1039/b719514a

structural information on the ternary species, ^{1}H and ^{31}P NMR measurements were performed over a wide pH range.

Experimental

Materials

The previously described ligands ***BMC*** and ***BPyC*** were prepared as white polychloride salt powders according to previously published procedures.[13] Elemental analyses were performed at the Service de Microanalyse, CNRS, 91198 Gif sur Yvette, France. Reagents were purchased from Acros Organics and from Aldrich Chemical Co.

Potentiometric titrations

Potentiometric measurements were performed in a jacketed cell thermostatted at 25.0 °C, kept under an inert atmosphere of purified argon, using an automatic titrator (Metrohm, DMS Titrino 716) connected to a microcomputer. The free hydrogen concentrations were measured with a glass-Ag/AgCl combined electrode (Metrohm) filled with 0.1 M NaCl. The electrode was calibrated in order to read $-\log[H^+]$, designated as pH, by titration of a small quantity of diluted HCl by standardized 0.02 M NaOH at 25 °C (and determining the equivalent point by Gran's method) followed by adjustment of the meter so as to minimize the calculated pH *vs.* observed values. $\log K_w$ for the system, defined in terms of $\log([H^+][OH^-])$, was found to be -13.78 at the ionic strength employed and was kept fixed during refinements.[14] As used in previous work, NaCl was employed as the supporting electrolyte to maintain the ionic strength at 0.10 M.

Potentiometric measurements of solutions containing equimolecular amounts of azaligands and the appropriate phosphate anion were made at about 1 mM in concentration and ionic strength $\mu = 0.10$ M (NaCl). Each titration utilised at least 10 points per neutralisation of a hydrogen ion equivalent and titrations were repeated until satisfactory agreement was reached. A minimum of three sets of data was used in each case to calculate the overall stability constants and their standard deviations. The standard deviations obtained for the different recognition constants are reported in Tables 1 and 2. The range of accurate pH measurements was considered to be 2–12. Equilibrium constants and species distribution diagrams were calculated by using HYPERQUAD 2003.[15]

The stability constants K_{alh} were noted with respect to ternary species $A_aL_lH_h$ where *a*, *l* and *h* are respectively the stoichiometric numbers of the anion (A) ligand (L) and the proton (H).

Table 1 Logarithms of protonation constants of related bismacrocycles and nucleotides. (H_2O; $I = 0.1$ M (NaCl); $T = 25.0 \pm 0.2$ °C; $[L]_{tot} = 10^{-3}$ M)[a]

	BMC	***BPyC***	***AMP***	***ADP***	***ATP***
[LH]/[L][H]	11.25(5)	11.08(1)	6.41(1)	6.56(2)	6.76(2)
$[LH_2]/[LH][H]$	10.02(2)	10.14(2)	3.75(1)	4.11(1)	4.31(2)
$[LH_3]/[LH_2][H]$	8.90(4)	8.97(4)	—	—	—
$[LH_4]/[LH_3][H]$	7.97(2)	7.84(5)	—	—	—
$[LH_5]/[LH_4][H]$	2.07(2)	2.30(5)	—	—	—

[a] Charges are omitted from the formulae for clarity; numbers in parentheses are standard deviations in the last significant figure.

Table 2 Logarithm recognition constants, $\log K_{alh}$, for the two bismacrocycles with ***AMP***, ***ADP***, and ***ATP*** ($I = 0.1$ M (NaCl); $T = 25$ °C)[a]

	AMP	***ADP***	***ATP***
BMC			
A + LH = ALH			
$A + LH_2 = ALH_2$	3.18(5)	2.44(1)	
$AH + LH = ALH_2$			
$A + LH_3 = ALH_3$	3.45(4)	2.59(3)	2.98(3)
$AH + LH_2 = ALH_3$			
$A + LH_4 = ALH_4$	3.91(4)	3.30(3)	3.73(4)
$AH + LH_3 = ALH_4$			
$A + LH_5 = ALH_5$			
$AH + LH_4 = ALH_5$	3.65(4)	2.91(3)	2.93(4)
$AH + LH_5 = ALH_6$			
$AH_2 + LH_4 = ALH_6$	4.11(4)	3.31(2)	3.26(4)
$AH_2 + LH_5 = ALH_7$	5.14(5)	3.65(4)	4.10(4)
BPyC			
A + LH = ALH		2.93(2)	
$A + LH_2 = ALH_2$	3.43(2)	3.41(2)	3.34(4)
$AH + LH = ALH_2$			
$A + LH_3 = ALH_3$	3.82(5)	4.06(6)	4.64(3)
$AH + LH_2 = ALH_3$			
$A + LH_4 = ALH_4$	4.17(4)	4.89(4)	5.64(3)
$AH + LH_3 = ALH_4$			
$A + LH_5 = ALH_5$			
$AH + LH_4 = ALH_5$	3.94(4)	5.01(4)	6.79(4)
$AH + LH_5 = ALH_6$			
$AH_2 + LH_4 = ALH_6$	4.10(5)	4.10(5)	4.10(5)
$AH_2 + LH_5 = ALH_7$	4.31(4)	5.76(3)	10.26(3)

[a] Charges omitted for clarity; numbers in parentheses are standard deviations in the last significant figure.

NMR measurements

^{1}H and ^{31}P NMR spectra in D_2O solutions at different pH values were recorded at 298 K with Bruker spectrometers. In ^{1}H NMR spectra, the reported peak positions are relative to HOD at 4.79 ppm. ^{1}H–^{1}H and ^{1}H–^{13}C 2D correlation experiments were performed to assign the signals. Small amounts of 0.01 M NaOD or DCl solutions were added to a solution of the chlorhydrated ligand to adjust the p[D]. The pH was calculated from the measured p[D] values with the following relationship: p[H] = p[D] − 0.40.[16]

Model study

The potential of the interaction of ***BPyC*** with ***ATP*** was modelled with the Spartan 2004 software (Semi-empirical/PM3 calculation).

X-Ray investigations

Single-crystal X-ray diffraction data were collected by François Michaud (Université de Bretagne Occidentale) at 170 K on an X-CALIBUR-2 CCD 4-circle diffractometer (Oxford Diffraction) with graphite-monochromatized MoKα radiation ($\lambda = 0.71073$ Å). Analysis of compound ***BPyC***: colourless rod-shaped crystals were obtained from an evaporated aqueous solution. Crystal data and structure refinement are summerized in Table 3. Unit-cell determination and data reduction, including interframe scaling, Lorentz, polarization, empirical absorption and detector sensitivity corrections, were carried out using programs attached to Crysalis software (Oxford Diffraction).[17] The structure was solved

Table 3 Crystal data[a] and structure refinement for $[\boldsymbol{BPyC}H_7]^{7+}$

Empirical formula	$C_{23}H_{64}Cl_7N_9O_7$: $(C_{23}H_{52}N_9)^{7+}$ $7Cl^- \cdot 6H_2O$
Formula weight/g mol^{-1}	826.98
Sample dimensions/mm	0.34 × 0.14 × 0.05 mm
Crystal system, space group	Monoclinic, $P2_1$
Z	2
a/Å	7.5917(5)
b/Å	17.7280(11)
c/Å	14.9620(10)
α/°	90
β/°	98.148(6)
γ/°	90
V/Å^3	1993.3(2)
T/K	170(2)
λ/Å	0.71073
μ/mm^{-1}	0.547
D_x/Mg m^{-3}	1.378
Measured reflections	15281
Unique reflections	7739; 5927 with $I > 2\sigma(I)$
$F(000)$	880
θ	2.94° < θ < 27.48°
$R_{int.}$	0.0339
h	−8 → 9
k	−22 → 21
l	−19 → 16
R_1 [$I > 2\sigma(I)$ and all data]	0.0482 and 0.0639
wR_2 [$I > 2\sigma(I)$ and all data]	0.1238 and 0.1323
S	0.972
w [$I > 2\sigma(I)$]	$1/[\sigma^2 + (0.0715P)^2]^b$
$\Delta\rho_{max}$/e Å^{-3}	1.146
$\Delta\rho_{min}$/e Å^{-3}	−0.282

[a] Refinement on all F^2, 436 parameters, 17 restraint, 7739 reflections with $I > 2\sigma(I)$. [b] $P = (F_o^2 + 2F_c^2)/3$

by direct methods and refined by the full-matrix least-squares method on F^2 with, respectively, the SIR92[18] and SHELXL 97[19] suites of programs. The hydrogen atoms were identified at the last step and refined under geometrical restraints and isotropic U-constraints.

Results and discussion

Ligand and substrate protonation

Potentiometric investigations. Protonation constants and species distribution diagrams of the ligands were reported and discussed in our previous paper[11] (Table 1 and ESI†). The two ligands contain four amino nitrogen atoms which behave as strong to moderate bases, and one which behaves as a weak base. The other protonation constants are not detected in the investigated p[H] range (2–12). It was deduced from potentiometric and NMR data that the first four protons occupy alternate positions separated either by a non-protonated amine group or by the linker. Moreover, the simultaneous downfield shift of the resonances of all the aliphatic protons indicates that on the NMR timescale the overall positive charges have an average homogeneous distribution over all the nitrogen atoms.

As regards the bis-2,6-pyridinylcyclen ***BPyC***, it presents a different protonation scheme below p[H] = 3 : the protonation of the nitrogen atom of the pyridine was evidenced in the $\boldsymbol{BPyC}H_5^{5+}$ species, whereas in the $\boldsymbol{BPyC}H_6^{6+}$ form, the six protons are symmetrically shared between the two macrocyclic subunits. Additionally, the crystal structure of the ***BPyC*** heptachlorhydride (Fig. 2, Table 3) shows, in the solid state, the further protonation of the nitrogen atom of the pyridine in the $\boldsymbol{BPyC}H_7^{7+}$ species.

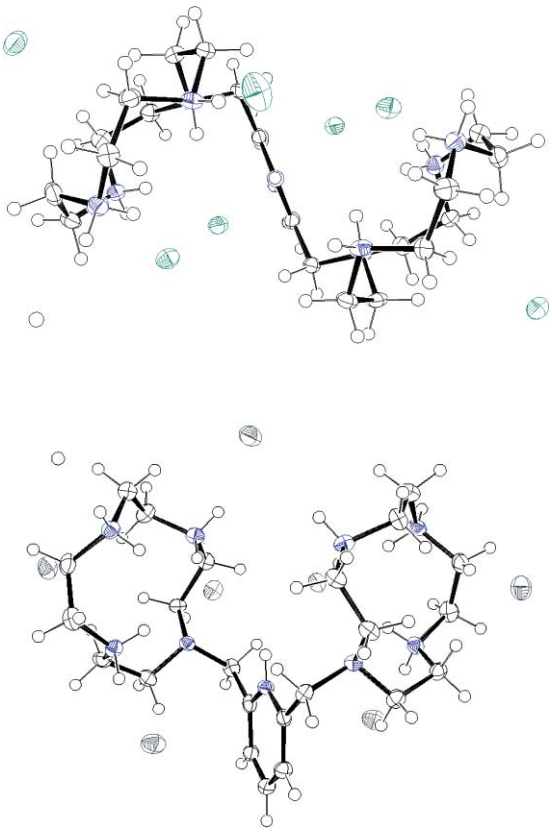

Fig. 2 ORTEP structure of $[\boldsymbol{BPyC}H_7]^{7+}$ with 50% probability ellipsoids.

Protonation constants (Table 1) of the nucleotides, measured according to our experimental conditions, are in good agreement with those of the literature. Species distribution diagrams for substrates ***AMP***, ***ADP*** and ***ATP***, deduced from their protonation constants, are presented in the ESI†.

Formation of ternary species

Potentiometric investigations. The potentiometric data of a solution containing equimolar amounts of ligand and anion are resolved, giving the $\log K_{alh}$ values for the species present in solution. Computer analysis by the HYPERQUAD[15] program furnished the overall equilibrium constants β_{alh} of the complexes formed by the adenosine-monophosphate, -diphosphate and -triphosphate (A) with the ligands (L), according to reaction (I) (charges omitted for simplicity). Once the number i of protons bound to the bismacrocyclic ligands (L) in the general $A_aL_lH_h$ complex is known, we can write the complexation reaction (II), according to the actual protonation state (charges omitted) and calculate log K_{alh}.

$$aA + lL + hH \rightleftharpoons A_aL_lH_h \quad \beta_{alh} \qquad (I)$$

$$AH_{(h-i)} + LH_i \rightleftharpoons ALH_h \quad K_{alh} \qquad (II)$$

Table 2 presents the logarithm of recognition constants, $\log K_{alh}$, for the ligands ***BMC*** and ***BPyC*** with the three nucleotide anions; ^{31}P NMR spectroscopy experiments showed that only complexes

with 1 : 1 anion–bismacrocycle stoichiometry were obtained in solution with ***AMP***, ***ADP*** and ***ATP***. The protonation constants of the anionic guests provide other possible sets of equilibria available to the formed ternary species; in each case, the most probable equilibrium corresponding to the major species simultaneously present is kept.

Fig. 3 presents plots of the logK_{alh} *versus* *h*H for the different ternary species with various degrees of protonation for selected systems.

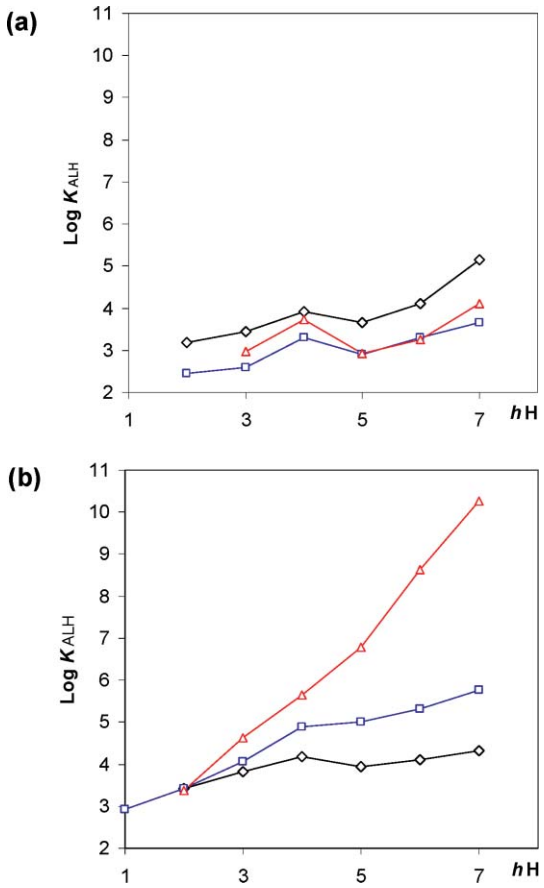

Fig. 3 LogK_{alh} *versus* *h*H (the different ternary species with various degrees of protonation) for (a) ***BMC***–nucleotide and (b) ***BPyC***–nucleotide systems (***AMP*** ◇, ***ADP*** □, ***ATP*** △).

The species distribution diagrams as a function of p[H] for the six anion–ligand systems were carried out and are represented in Fig. 4 for ***BMC***–, ***BPyC***–***ATP*** (for the others, see the ESI†), and the percentage of complexed ALH_h species in Fig. 5. In sharp contrast to the ***BMC***–nucleotide system, the ***BPyC***-based species always dominate over the p[H] range. One can note an increase in the binding constants as the number of protons on the bis-macrocycle increases to a maximum of seven, corresponding to a penta-protonated host and a di-protonated guest. As observed for the previously described inorganic phosphate–biscyclen systems, the higher recognition constants are also obtained here for the triphosphate species.[11,12] It is evident that for the same degree of protonation of the ligand, ***ATP*** presents more negatively charged oxygen atoms for hydrogen bond formation. Except for ***BPyC***–***ATP***, a slight decrease was observed as the consequence of the first protonation of the phosphate anion in ALH_5 species. The

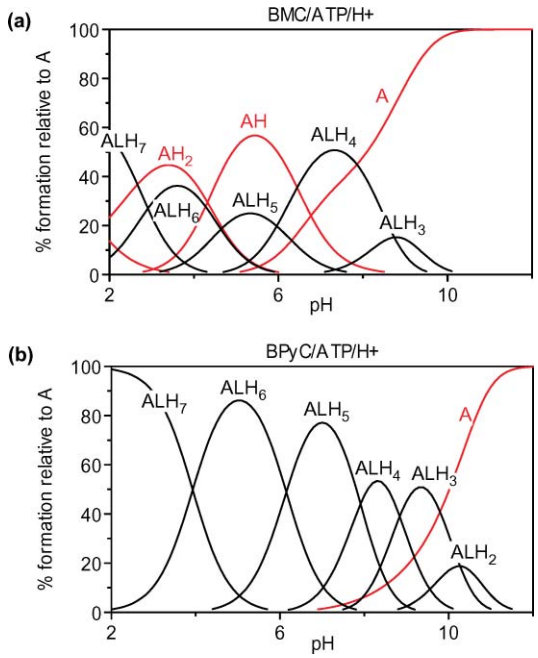

Fig. 4 Species distribution diagrams for ***ATP*** with (a) ***BMC*** and (b) ***BPyC*** as a function of p[H].

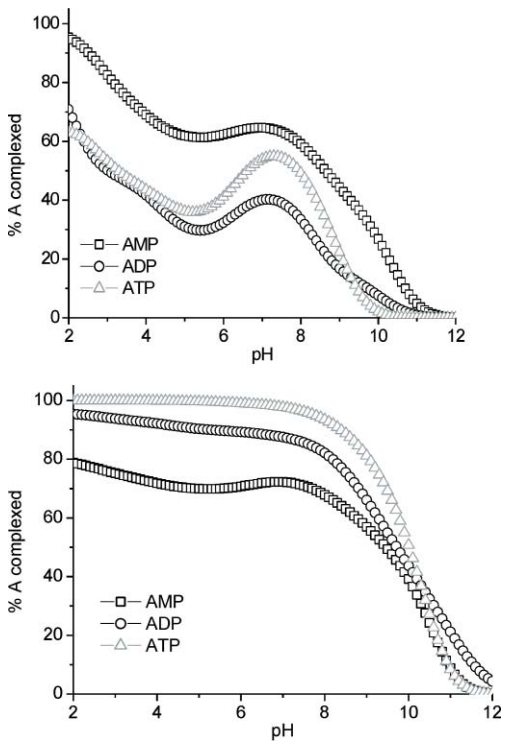

Fig. 5 Overall percentages of complexed ALH_h species with ***BMC*** (top) and ***BPyC*** (bottom) as function of p[H]. Percentages are calculated with respect to anions.

high recognition constants reported for this system are certainly related to the presence of the pyridine group, which interacts with the guest over the whole p[H] range. More generally, from the point of view of their recognition constants, the nucleotides and phosphate anions bind to the ligands ***BMC*** and ***BPyC*** in a similar manner, except ***AMP***, which (compared to ***ADP*** and ***ATP***) gives

the best complexation constants with ***BMC***, as already observed with the orthophosphate anion and similar ligands.[11]

Considering the overall percentages of complexed ALH_h species as a function of p[H] (Fig. 5), one can note the high complexation rate of ***BPyC–ATP*** up until p[H] 9, at which point it quickly decreases as the number of ammonium sites becomes insufficient to induce efficient host–guest interaction. One can note also that, compared to ***BMC***, the presence of the pyridinyl moiety in ***BPyC*** constitutes in any case a benefit for the formation of ternary species, certainly due to the possibility of supplementary hydrogen bonding offered by the nitrogen atom of the linker.

NMR investigations

In order to localize the protonation sites of the anion, ^{1}H and ^{31}P NMR spectra, as a function of p[H], were recorded in aqueous D_2O/DCl or NaOD solutions (Fig. 6). Special interest was focused on the ***ATP*** anion, which gives the higher recognition constants.

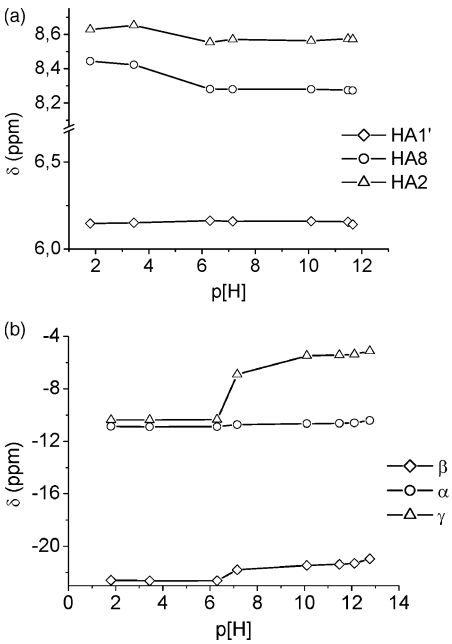

Fig. 6 (a) ^{1}H NMR and (b) ^{31}P NMR shifts of the ***ATP*** protons and phosphorus atoms between p[H] 2 and 13 (D_2O; $T = 25\,^{\circ}C$; 300.135 MHz (^{1}H NMR), 121.498 MHz (^{31}P NMR); $[\boldsymbol{ATP}] = 5.5 \times 10^{-3}$ M).

The first protonation of this nucleotide ($K_{101} = 6.76$) was observed on the ^{31}P NMR spectra, which revealed a downfield shift of the γ phosphorus signal between p[H] 6 and 7 corresponding to the protonation of the γ terminal phosphate group. The second one ($K_{102} = 4.31$), appeared on the ^{1}H NMR spectra, which presented a downfield shift of signals attributed to the H_{A2} and H_{A8} protons of the adenine part between p[H] 4–6, while $H_{A1'}$ remained unchanged. This result is consistent with a proton shared between the three nitrogen atoms N_{A3}, N_{A1} and N_{A7} of the adenine moiety, except for N_{A9}, which gives its electron pair to the aromatic system. The other protonation constants are two low (<2) to be detected.

Anion complexation was also monitored by recording ^{1}H NMR spectra on a solution containing host and guest in 1 : 1 molar ratio at different p[H] values. Figs. 7 and 8 show the p[H] dependence of the signals of the protons of the hosts, ***BMC*** and ***BPyC***, free or

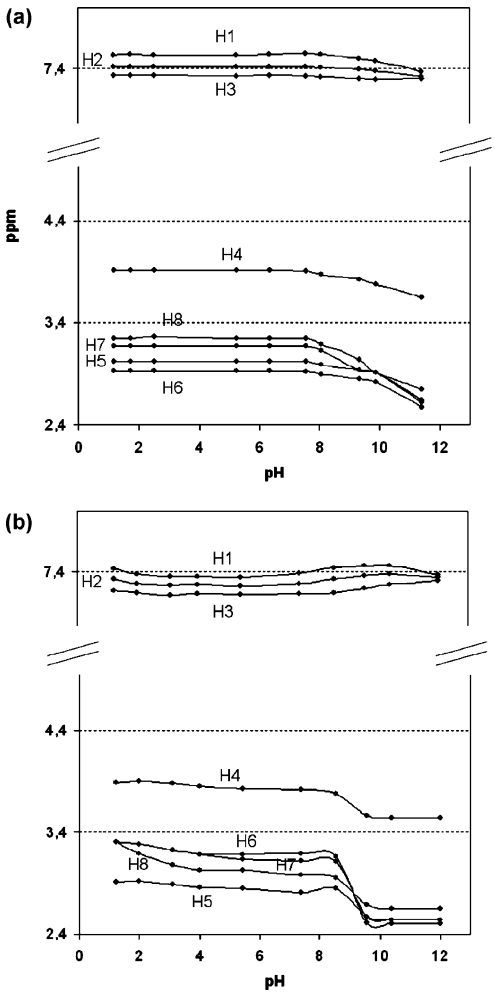

Fig. 7 Experimental ^{1}H chemical shifts for the proton of the ***BMC*** ligand (a) free and (b) in the presence of ***ATP*** (D_2O; $T = 25\,^{\circ}C$; 300.135 MHz, $[A] = [L] = 0.02$ M).

in presence of their guest ***ATP***. For clarity, the p[H] dependence of the signals of the protons of ***ATP***, free and in the presence of ***BMC*** and ***BPyC***, are reported separately in Fig. 9.

Significant upfield displacements are observed for the resonances of the adenine protons H_{A2}, H_{A8}, and the anomeric proton $H_{A1'}$ of the nucleotide (Fig. 9), as well as the aromatic protons H_1, H_2, and H_3 (Figs. 7 and 8) of the bismacrocycle linkers in the p[H] range 2–10. Moreover, this behaviour was not observed on the aromatic protons of the bismacrocycle linkers with inorganic triphosphate (see ESI†). These observations are consistent with the participation of π-stacking interactions[9e] between the aromatic spacer and the adenine moiety in the stabilization of the ternary species which would give a face-to-face disposition in the complex. One can note also in the complex the upfield shift of the H_8 signal (deprotonation of N_3), the downfield shift of H_6 signal (protonation of N_2), and to a lower extent H_7, which indicates that N_2 and N_4 are more implicated in the binding system of the complex (Figs. 7 and 8).

The behaviour of ***BPyC–ATP*** ternary species in acidic medium, below p[H] 4, is remarkable (Fig. 8b): the strong downfield shifts observed simultaneously for the aromatic H_1 and H_2 protons and H_4 imply the strong participation of the linker in the structure of

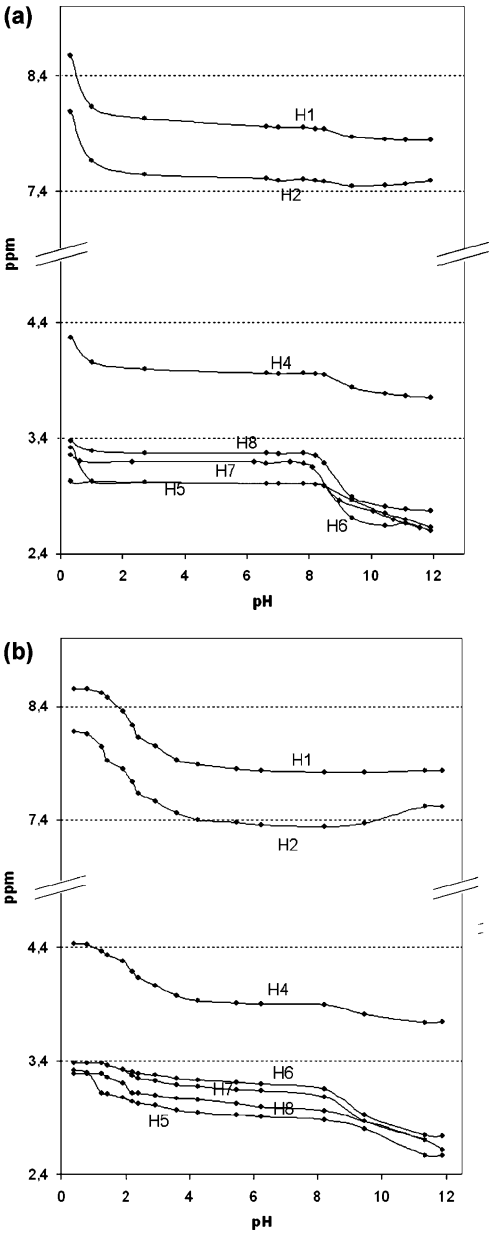

Fig. 8 Experimental ^{1}H chemical shifts for the proton of the ***BPyC*** ligand (a) free and (b) in the presence of ***ATP*** (D_2O; $T = 25$ °C; 300.135 MHz, [A] = [L] = 0.02 M).

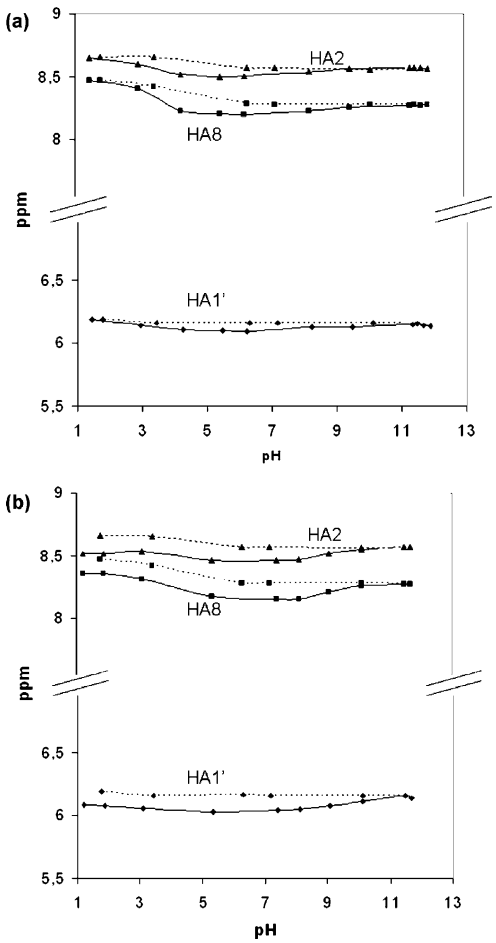

Fig. 9 Experimental ^{1}H chemical shifts for the $H_{A1'}$, H_{A2} and H_{A8} protons of free ***ATP*** (dotted lines) and ***ATP*** in the presence of ligands (plain lines): (a) ***BMC*** and (b) ***BPyC***.

Table 4 $\Delta\delta$ Shifts ($\delta_{\text{free anion}} - \delta_{\text{complex}}$) of the ^{31}P NMR signal of the ***ATP*** anion, free or in the presence of the ***BMC*** or ***BPyC*** ligands at various p[H]

	$-\Delta\delta$/ppm					
	p[H] = 1		p[H] = 4		p[H] = 10	
	BMC	***BPyC***	***BMC***	***BPyC***	***BMC***	***BPyC***
P_α	0.02	0	−0.04	0.06	0.03	0
P_β	0.38	0.03	0.36	0.25	0.11	0.09
P_γ	0.02	0.01	0.05	0.04	0.05	0.01

the complex. At the same time, one can observe the disappearance of the upfield displacements of the adenine protons concerned by the π-stacking interactions (Fig. 8b and Fig. 9b).

The changes of the ^{31}P NMR chemical shifts of ***ATP*** upon complexation by ***BMC*** and ***BPyC*** present also some interesting features (Table 4). The spectrum exhibits a triplet for the central phosphorus atom (P_β) and a two doublets for the lateral phosphorus atoms (P_α and P_γ) around −21 ppm, −10 ppm and −5 ppm respectively at p[H] 12.

One can assume that the supplementary upfield shift for the triplet (P_β) observed at p[H] 4 is certainly due to the insertion of the anion inside the intercyclic space delimited by the two cyclen moieties of ***BMC*** and ***BPyC*** in relation to the magnetic anisotropy due to the aromatic moieties. As a matter of fact, the central phosphorus atom is well situated in front of the benzene ring and therefore is fully exposed to its shielding zones, whereas the lateral atoms (P_α and P_γ) are subjected to a smaller effect.

These observations lead us to conclude that the phosphate part lies in parallel between the two cyclen cores of the ligand ***BMC*** or ***BPyC***: P_γ and P_β form hydrogen bonds with N_2 and N_4 respectively and P_α contributes to the stability of the structure through supplementary π-stacking interactions due to its organic aromatic moiety; hence P_β is the more exposed to the shielding zone of the aromatic part of the linker. It is noteworthy that above p[H] 4 the behaviour of the two different linkers is very similar.

At p[H] 1 this situation is maintained for ***BMC*** whereas for ***BPyC*** the supplementary upfield shift for the triplet (P_β) observed at p[H] 4 disappears, in correlation with the protonation of the pyridine nitrogen atom of the linker, clearly indicated by the shifts of the aromatic protons of the linker and H_4 signal. One can imagine that the protonation of the linker involves its participation in the binding process by an additional point of attachment which certainly concerns the neighbouring P_α. This strong interaction, corroborated by an enhanced recognition constant, implies the rotation of the pyridine linker and consequently the disappearance of the weaker π-stacking interactions. Moreover, the electrostatic repulsions between protonated adenine and pyridine rings contribute also to the non-stacked open structure adopted by the adduct at acidic p[H]. In this new situation, P_β (like P_α and P_γ) is not exposed to the shielding zone of the adenine part; the rest of the complex remains certainly unchanged, as indicated by the weak variations of the chemical shifts of the protons of the cyclen cores.

These results call for a comparison with our previous studies concerning inorganic phosphate anion.[11] We deduced from the protonation sequence of the cyclen cores that for triphosphate anion, the two lateral phosphorus atoms, which coordinate mainly with N_2, N_3 and N_4, were the more implicated in the structure of the complex. Subsequently, the protonated pyridine interacted with the central phosphorus atom. Here, with ***ATP***, the structure of the ternary species is somewhat different and P_α is more probably involved with the supplementary binding site offered by the protonated pyridine when protonated in acidic medium.

Possible host–guest networks can be deduced from this observation and are presented in Fig. 10. One can assume that they should be also applicable to ***AMP*** and ***ADP***, for which the protonation of the linker involves also stronger recognition constants.

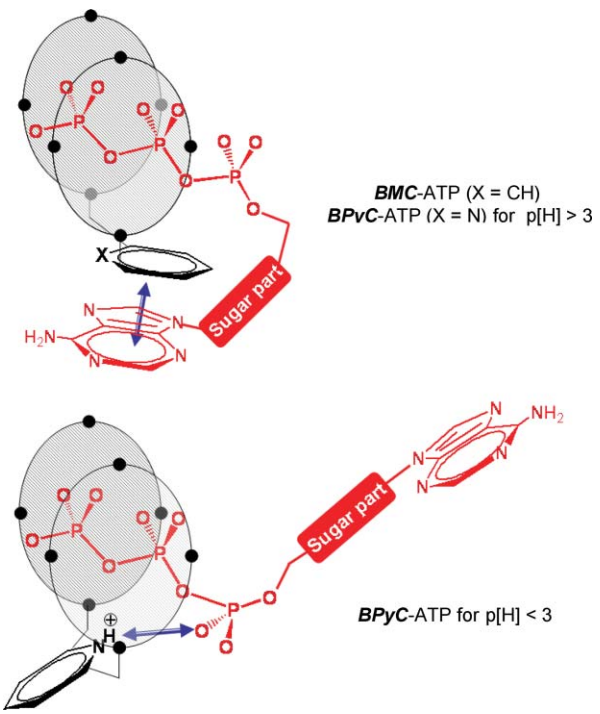

Fig. 10 Proposed structure for ***BMC–ATP*** and ***BPyC–ATP*** complexes depending on the p[H] range (H-bonds and charges with cyclen moieties are omitted for clarity).

From the locations of protons suggested by NMR experiments, we carried out computer-generated representations of the ***BPyC–ATP*** complex (ALH_7). Fig. 11 highlights the good ligand–anion association and the benefit of a supplementary central point of attachment. This model is in good agreement with our experimental findings.

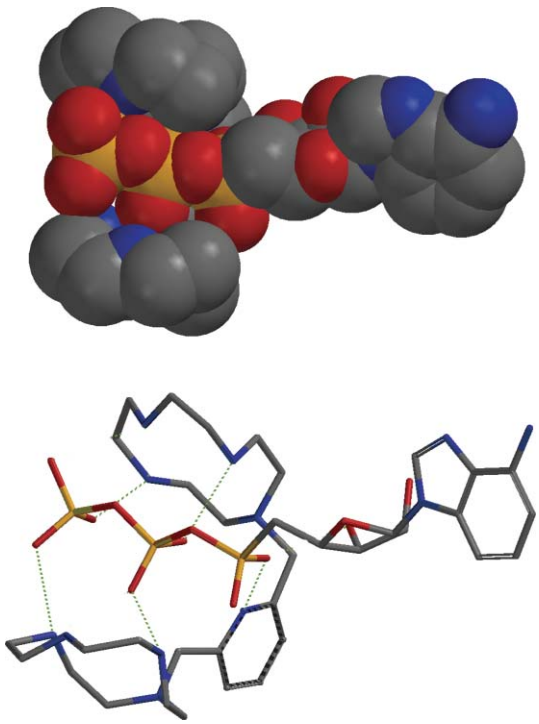

Fig. 11 Proposed model for the interaction of the protonated form of ***BPyC*** with ***ATP*** (ALH_7).

Conclusion

In this continuation of our previous work on inorganic phosphate anions,[11,12] we have shown that cyclen-based bismacrocycles ***BMC*** and ***BPyC*** also present interesting features in their interaction with nucleotides ***AMP***, ***ADP*** and ***ATP***. Compared to inorganic phosphates, supplementary π-stacking interactions contribute unambiguously to the recognition process; however, coulombic interactions and hydrogen bonding constitute the driving forces for high binding constants. Here also, at around p[H] 2, the additional central anchoring group of ***BPyC*** allows the ligand to interact more efficiently with the phosphate moiety of the ***AMP***, ***ADP*** and ***ATP*** nucleotide species.

Taking into account the results obtained with linear octaamines and inorganic phosphates,[12c] it would be interesting to compare these cyclen-based bismacrocycles with their open linear octaamine analogues for nucleotide recognition.

Acknowledgements

This research work was supported by the Ministère de l'Education Nationale et de la Recherche and by the Comité National pour la Recherche Scientifique. We also thank Nelly Kervarec for her contribution to the 2D NMR measurements.

References

1 (*a*) P. D. Beer, *Acc. Chem. Res.*, 1998, **31**, 71; (*b*) P. D. Beer and P. A. Gale, *Angew. Chem., Int. Ed.*, 2001, **40**, 487; (*c*) A. Bianchi, K. Bowman-James and E. García-España, *Supramolecular Chemistry of Anions*, John Wiley & Sons, Chichester, UK, 1997.

2 O. A. Gerasimchuk, S. Mason, A. M. Llinares, M. Song, N. W. Alcock and K. Bowman-James, *Inorg. Chem.*, 2000, **39**, 1371.

3 J. Wang, A. E. Martell and R. J. Motekaitis, *Inorg. Chim. Acta*, 2001, **322**, 47.

4 C. Anda, A. Llobet, A. E. Martell, B. Donnadieu and T. Parella, *Inorg. Chem.*, 2003, **42**, 8545.

5 Z. F. Kanyo and D. W. Christianson, *J. Biol. Chem.*, 1991, **266**, 4264.

6 M. V. Rekharsky and Y. Inoue, *J. Am. Chem. Soc.*, 2002, **124**, 813.

7 S. Aoki and E. Kimura, *Rev. Mol. Biotechnol.*, 2002, **90**, 129.

8 C. Bazzicaluppi, A. Bencini, A. Bianchi, L. Borsari, C. Giorgi and B. Valtancoli, *J. Org. Chem.*, 2005, **70**, 5257.

9 (*a*) M. W. Hosseini and J.-M. Lehn, *Helv. Chim. Acta*, 1987, **70**, 1312; (*b*) B. Dietrich, M. W. Hosseini and J.-M. Lehn, *Helv. Chim. Acta*, 1985, **68**, 289; (*c*) C. Bazzicaluppi, A. Bencini, A. Bianchi, M. Cecchi, B. Escuder, V. Fusi, E. García España, C. Giorgi, S. V. Luis, C. Maccagni, V. Marcelino, P. Paoletti and B. Valtancoli, *J. Am. Chem. Soc.*, 1999, **121**, 6807; (*d*) C. Anda, A. Llobet, V. Salvadó, A. E. Martell and R. J. Motekaitis, *Inorg. Chem.*, 2000, **39**, 3000; (*e*) C. Anda, C. Bazzicalupi, A. Bencini, E. Berni, A. Bianchi, P. Fornasari, A. Llobet, C. Giorgi, P. Paoletti and B. Valtancoli, *Inorg. Chim. Acta*, 2003, **356**, 167; (*f*) Y. H. Guo, Q. C. Ge, H. Lin, H. K. Lin and S. R. Zhu, *Polyhedron*, 2002, **21**, 105; (*g*) E. García España, P. Diaz, J. M. Llinares and A. Bianchi, *Coord. Chem. Rev.*, 2006, **250**, 2952.

10 (*a*) M. M. Rosenkilde, L. O. Gerlach, S. Hatse, R. T. Skerlj, D. Schols, G. J. Bridger and T. W. Schwartz, *J. Biol. Chem.*, 2007, **282**(37), 27354; (*b*) E. De Clercq, *Mini-Rev. Med. Chem.*, 2005, **5**(9), 805; (*c*) G. A. Donzella, D. Schols, S. W. Lin, J. A. Este, K. A. Nagashima, P. J. Maddon, G. P. Allaway, T. P. Sakmar, G. Henson, E. De Clercq and J. P. Moore, *Nat. Med.*, 1998, **4**, 72.

11 S. Develay, R. Tripier, M. Le Baccon, V. Patinec, G. Serratrice and H. Handel, *Dalton Trans.*, 2005, 3016.

12 (*a*) S. Develay, R. Tripier, M. Le Baccon, V. Patinec, G. Serratrice and H. Handel, *Dalton Trans.*, 2006, 3418; (*b*) S. Develay, R. Tripier, N. Bernier, M. Le Baccon, V. Patinec, G. Serratrice and H. Handel, *Dalton Trans.*, 2007, 1038; (*c*) N. Le Bris, H. Bernard, R. Tripier and H. Handel, *Inorg. Chim. Acta*, 2007, **360**, 3026.

13 M. Le Baccon, F. Chuburu, L. Toupet, H. Handel, M. Soibinet, I. Deschamps-Olivier, J. P. Barbier and M. Aplincourt, *New J. Chem.*, 2001, **25**, 1168.

14 (*a*) G. Gran, *Analyst*, 1952, **77**, 661; (*b*) A. E. Martell and R. J. Motekaitis, *Determination and Use of Stability Constants*, 2nd edn, John Wiley and Sons, New York, 1992.

15 P. Gans, A. Sabatini and A. Vacca, *Talanta*, 1996, **43**, 1739.

16 P. K. Glasoe and F. A. Long, *J. Phys. Chem.*, 1960, **64**, 188.

17 *Crysalis software system*, Oxford Diffraction Ltd, version 1.171.28cycle4β, 2005.

18 A. Altomare, G. Cascarano, C. Giacovazzo and A. Guagliardi, 'SIR 92 – A program for crystal structure solution', *J. Appl. Crystallogr.*, 1993, **26**, 343.

19 G. M. Sheldrick, *SHELXL-97, Program for refinement of crystal structures*, University of Göttingen, Germany, 1997.